European Journal of Pharmaceutical Sciences 96 (2017) 398–410

Contents lists available at ScienceDirect

European Journal of Pharmaceutical Sciences

journal homepage: www.elsevier.com/locate/ejps

Very fast dissolving acid carboxymethylcellulose-rifampicin matrix: Development and solid-state characterization

Laura C. Luciani-Giacobbe [a], María V. Ramírez-Rigo [b,c], Yamila Garro-Linck [d], Gustavo A. Monti [d], Ruben H. Manzo [a], María E. Olivera [a,*]

[a] Unidad de Investigación y Desarrollo en Tecnología Farmacéutica (UNITEFA), CONICET and Departamento de Farmacia, Facultad de Ciencias Químicas, Universidad Nacional de Córdoba, Ciudad Universitaria, 5000 Córdoba, Argentina
[b] Planta Piloto de Ingeniería Química (PLAPIQUI), CONICET and Departamento de Ingeniería Química, Universidad Nacional del Sur, Camino La Carrindanga Km 7, 8000 Bahía Blanca, Argentina
[c] Departamento de Biología, Bioquímica y Farmacia, Universidad Nacional del Sur, San Juan 670, 8000 Bahía Blanca, Argentina
[d] Instituto de Física Enrique Gaviola (IFEG), CONICET and Facultad de Matemática, Astronomía y Física, Universidad Nacional de Córdoba, Ciudad Universitaria, 5000 Córdoba, Argentina

ARTICLE INFO

Article history:
Received 8 May 2016
Received in revised form 23 September 2016
Accepted 5 October 2016
Available online 6 October 2016

Keywords:
Drug delivery
Crystalline solid dispersion
Zwitterion
Rifampicin
Wetting
Dissolution rate
Solid-state properties

ABSTRACT

One of the main obstacles to the successful treatment of tuberculosis is the poor and variable oral bioavailability of rifampicin (RIF), which is mainly due to its low hydrophilicity and dissolution rate. The aim of this work was to obtain a hydrophilic new material that allows a very fast dissolution rate of RIF and therefore is potentially useful in the development of oral solid dosage forms.

The acid form of carboxymethylcellulose (CMC) was co-processed with RIF by solvent impregnation to obtain CMC-RIF powder, which was characterized by polarized optical microscopy, powder x-ray diffraction, DSC-TGA, hot stage microscopy, ^{13}C and ^{15}N solid-state NMR and FT-IR spectroscopy. In addition, the CMC-RIF matrices were subjected to water uptake and dissolution studies to assess hydrophilicity and release kinetics.

CMC-RIF is a crystalline solid dispersion. Solid-state characterization indicated that no ionic interaction occurred between the components, but RIF crystallized as a zwitterion over the surface of CMC, which drastically increased the hydrophilicity of the solid. The CMC-RIF matrices significantly improved the water uptake of RIF and disintegrated in a very short period immediately releasing RIF. As CMC improves the hydrophilicity and delivery properties of RIF, CMC-RIF is very useful in the design of oral solid dosage forms with very fast dissolution of RIF, either alone or in combination with other antitubercular drugs.

1. Introduction

Tuberculosis (TB) is a very important infectious disease worldwide. In 2014, 9.6 million people became ill with TB and 1.5 million died from the disease (WHO, 2015). Currently, a long-term combined therapy with first-line drugs is used for the treatment of TB, with rifampicin (RIF, Fig. 1) and isoniazid being administered for six months and supplemented with ethambutol and pyrazinamide during the first two months (Ma et al., 2010). Oral solid RIF formulations are available as immediate release solid oral dosage forms (tablets or capsules) containing RIF alone or combined with other anti-TB drugs.

One of the main obstacles to the successful treatment of TB is the poor and variable oral bioavailability of RIF, which is a class II drug in the Biopharmaceutics Classification System (BCS), implying that the rate and extent of dissolution play an important role in the *in vivo* performance. RIF is an amphoteric compound freely soluble at pH values below 3 but only slightly soluble at pH values between 3 and 8. Thus, *in vivo* dissolution of RIF in the acidic environment of the stomach is a necessary condition for its bioavailability (Panchagnula et al., 2007) since it is mainly absorbed in the stomach and duodenum (Mariappan and Singh, 2003).

There are several bioinequivalence reports about RIF and numerous causes for the non-equivalence of RIF oral formulations have been postulated (Becker et al., 2009). For instance, RIF pH-dependent solubility, hydrophobicity and the crystalline state lead to differences in wettability and the dissolution rate. The influence of excipients in the performance of the solid dosage form and inter-individual variability in RIF absorption and the metabolism are also associated with RIF bioavailability problems with the degradation of RIF in the acidic gastric media also being important (Becker et al., 2009). Sub-therapeutic plasma levels of RIF may increase the risk of resistance in view of the fact that its activity is highly dose-dependent and that RIF resistance mechanism develops in only one step (Ellard and Fourie, 1999; Jindani et al., 1980; Telenti et al., 1993).

Some promising research has been carried out with the aim of improving RIF performance, such as amorphization, particle size reduction

* Corresponding author at: Haya de la Torre y Medina Allende, Edificio Ciencias 2, Ciudad Universitaria, 5000 Córdoba, Argentina.
E-mail address: meoliver@fcq.unc.edu.ar (M.E. Olivera).

http://dx.doi.org/10.1016/j.ejps.2016.10.013
0928-0987/

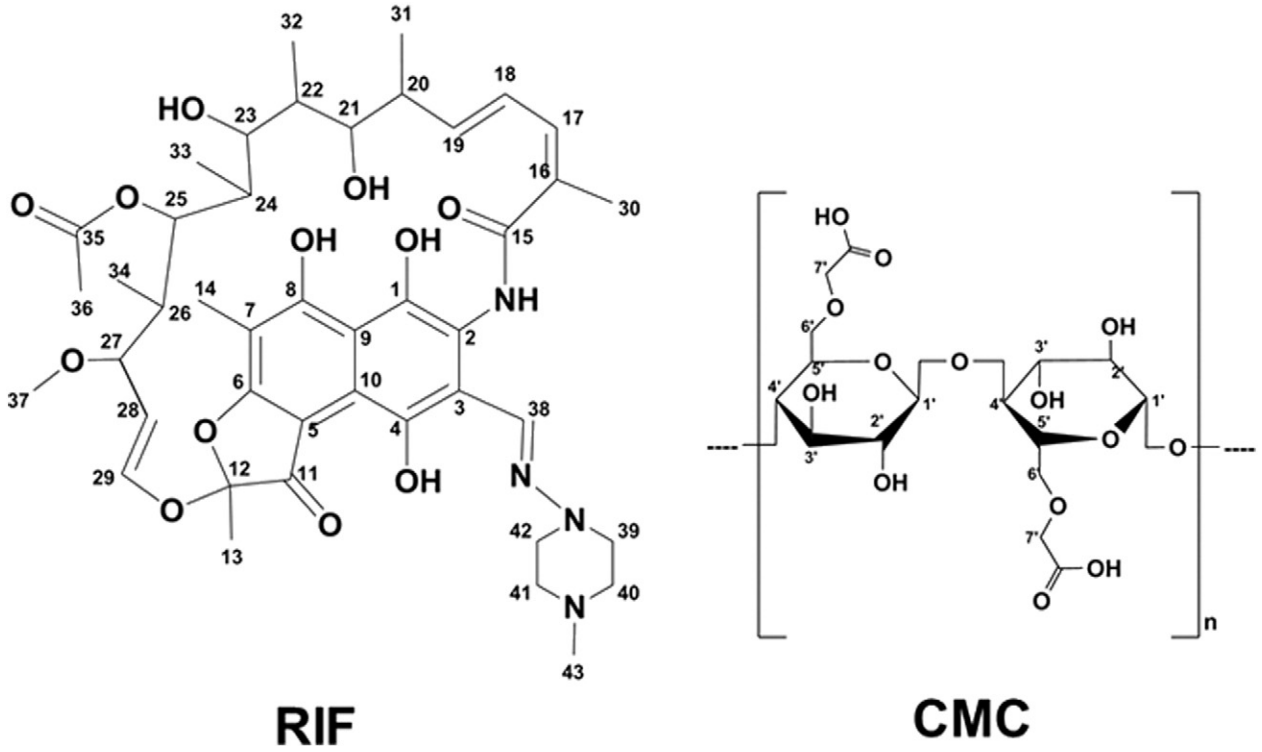

Fig. 1. Molecular structure of rifampicin (RIF) and carboxymethylcellulose (CMC) monomer. The numbering system of RIF is in agreement with the special nomenclature of rifamycins.

or RIF encapsulation in liposomes or polymers (Henwood et al., 2001; Singh et al., 2014; Schianti et al., 2013). However, these techniques use additives that are not approved by health organizations and which usually increase the production costs (Pandey and Ahmad, 2011). Moreover, high oral doses of RIF (300 mg) and the need to combine it with fixed doses of other anti-TB drugs represents an additional challenge. Consequently, the development of new materials capable of overcoming these drawbacks of RIF and therefore useful in the preparation of oral solid formulations with simple and low-cost procedures may provide a new approach for developing new effective anti-TB dosage forms.

Carboxymethylcellulose in its acid form (CMC, Fig. 1) is water insoluble, behaving as an ionic exchange resin that may be easily loaded with drug molecules having readily protonated basic groups to yield insoluble products. In fact, CMC-complexes with some basic model drugs have shown very rapid release in acidic media and have been proposed as a platform to increase the dissolution rate of drugs with poor aqueous solubility (Ramírez Rigo et al., 2004; Ramírez Rigo et al., 2009). Thus, the hypothesis of this work was that formulation of RIF on a CMC carrier would enable the development of oral solid dosage forms with very rapid RIF dissolution rate.

2. Materials

RIF (Pharmaceutical grade) and KBr (spectroscopic grade) were purchased from Parafarm®-Argentina and Merck®-Germany, respectively. CMC-Na (ultra-high viscosity, highly purified, degree of substitution (COOH) 0.98) was purchased from Fluka®-Argentina, with a 1% w/v CMC-Na aqueous solution having a viscosity of 2100 mPa.

CMC was obtained by adding 37% HCl (Cicarelli®-Argentina) to an aqueous hydrogel of 3.6% CMC-Na until pH = 2, and further precipitation of CMC was carried out with ethanol. The solid was separated by filtration, washed with water, filtered, and dried in an oven at 50 °C to constant weight. The product was milled and sieved through 40# and 70# mesh sieves. The equivalents of carboxylic groups per gram of CMC were assayed by acid-base titration, as previously described in Ramírez Rigo et al. (2009). Briefly, 15 mg of CMC were dissolved with 3 mL of 0.05 M NaOH. After that, 30 mL of distilled water were added to the system and titrated with 0.05 M HCl to the equivalent point. The equivalents of carboxylic groups per gram of CMC were 3.75×10^{-3}. This assay was performed in triplicate.

All other chemicals and reagents used were of pharmaceutical or analytical grade and used as received.

3. Methods

3.1. Preparation of CMC-RIF

CMC-RIF was prepared in a mortar by the addition of 12 mL of ethanol to a mixture of 1 g of CMC and 3.09 g of RIF (1:1 M ratio of carboxylic equivalents in CMC: amine groups of RIF). The resulting semi-solid paste was subjected to kneading during 5 min and left overnight at room temperature. The mass was then extruded using a 30# mesh sieve (ASTM, Zonytest, Argentina) to obtain granules that were dried to constant weight in an oven at 40 °C.

CMC-$RIF_{0.8}$ and CMC-$RIF_{0.6}$ were prepared by the same procedure from 1:0.8 and 1:0.6 CMC:RIF molar ratios.

A physical mixture of CMC + RIF with a composition equivalent to CMC-RIF was also prepared for comparative purposes by a simple mixing of the powders. For a better understanding of the thermal behavior, a CMC + RIF·$2H_2O$ physical mixture was also obtained.

3.2. RIF Content in CMC-RIF

The RIF percentage in CMC-RIF was determined in the solid material and after its dispersion in acidic media with the content of RIF in the solid material being calculated thorough total nitrogen quantification using the Kjeldahl method (AOAC Official Method 991.20, 2005). In addition, the nitrogen content of a pure RIF sample was used as a

reference. The RIF percentage in the solid was calculated according to the following equation:

$$RIF_{(CMC\text{-}RIF)}(\%) = \frac{N_{(CMC\text{-}RIF)}(\%)}{N_{(RIF)}(\%)} \times 100 \quad (1)$$

where $N_{(CMC\text{-}RIF)}$ (%) is the percentage of nitrogen in CMC-RIF and $N_{(RIF)}$ (%) is the percentage of nitrogen in the pure RIF sample.

In order to determine the RIF available after dispersion of CMC-RIF in an acidic medium, approximately 30 mg of CMC-RIF were exactly weighed and transferred to a 100 mL volumetric flask and HCl 0.1 M preheated to 37 °C was added. The sample was then subjected to ultrasonic vibration for 5 min to allow RIF release from the granules, since CMC is not soluble in water. Finally, 1 mL of the supernatant was diluted to 10 mL with USP phosphate buffer pH 6.8 and RIF was quantified by an HPLC stability-indicating method according to Sankar et al. (2003). This assay was performed in duplicate.

3.3. Solid State Characterization of CMC-RIF

The following experiments were performed on CMC-RIF, the starting materials and the physical mixture CMC + RIF, with the methods being detailed below:

3.3.1. Polarized Optical Microscopy

Optical images of the samples were taken using an Olympus BX41 microscope (Bio Analítica Argentina S.A., USA) equipped with an Infinity 1 digital camera. Image analysis was performed using Infinity Analyze software.

3.3.2. Powder X-ray Diffraction (p-XRD)

The p-XRD patterns were acquired at room temperature on an X-ray diffractometer (PANalytical X'Pert Pro, Holland) using Cu Kα radiation (tube operated at 40 kV, 100 mA). Data were collected over an angular range from 5 to 35° 2θ in continuous scan mode, with a step size of 0.05° 2θ and a time counting of 5 s per step. The obtained diffractograms were analyzed by an X'Pert data viewer (PANanalytical, Holland).

3.3.3. Thermal Analysis

The samples were subjected to differential scanning calorimetry (DSC) and thermogravimetric analysis (TGA), with data collected using a thermal analyzer over a temperature range of 30–300 °C. A DSC standard cell of an A2920 MDSC (TA Instruments, USA) equipped with a data station (Universal Analysis, TA Instruments) was used to determine the DSC curves. The temperature axis and the cell constant of the DSC cell were calibrated with indium (15.52 mg, 99.99% pure, peak maximum at 156.71 °C, Aldrich, Milwaube, USA). The samples (0.8–2.0 mg) were heated in aluminum pans under nitrogen flux (50 mL/min) and run at 10 °C/min ramps in crimped pans. The fusion, dehydration, vaporization and decomposition temperatures were taken as the extrapolated onset temperature of the endothermic/exothermic peak. Additionally, RIF·$2H_2O$ and CMC + RIF·$2H_2O$ physical mixture samples were heated from room temperature to 80 °C and maintained at that temperature for 1 min to eliminate water adsorbed onto particle surfaces. After that, the samples were cooled and scanned for a second time in the conditions described above. Using a 2950 TGA HR thermogravimetric analyzer (TA Instruments) linked to a data station, the TGA temperature axes were calibrated with the Curie point of Ni (354.3 °C). Other samples (0.8–1.3 mg) were placed in open aluminum pans and heated under the same conditions used in DSC analysis. The amount of water contained in the samples was directly obtained from the y-axis of the thermogram, which represented the weight loss until the end of the first step of the dTGA. Hot stage microscopy (HSM) was carried out on a hot stage microscope (Leitz Wetzlar, Germany) provided with a digital thermometer. Several crystals were immersed in mineral oil, covered with a cover slip and heated at a rate of 10 °C/min. This technique allows vapor bubbles to be observed when water is released from the surface of a solid particle and shape modifications that can be related to solid-solid phase transitions (Chadha et al., 2012).

3.3.4. ^{13}C and ^{15}N Solid State Nuclear Magnetic Resonance (NMR)

High-resolution solid-state ^{13}C and ^{15}N cross polarization/magic angle spinning (CP-MAS) NMR experiments were performed on a Bruker Avance II spectrometer at a Larmor frequency of 300.13 MHz, 75.46 MHz and 30.42 MHz for ^{1}H, ^{13}C and ^{15}N, respectively, equipped with a 4 mm MAS probe. All samples were spun at 10 kHz, and the ^{13}C CP-MAS spectra were recorded using a variable amplitude ramped CP pulse of 2 ms. The ^{13}C quaternary carbon edition experiment (Non Quaternary Suppression, NQS) was performed on all the samples, which enabled the quaternary carbon signals and methyl groups to be identified, thereby permitting the accurate assignment of the signals (Harris, 1994).

For the ^{15}N CP-MAS experiment, the amplitude ramped CP pulse was 6 ms with ^{1}H-^{15}N short contact time (SCT) CP-MAS experiments being recorded for RIF and CMC-RIF using a CP contact time of 200 μs. Glycine was used as an external reference for the ^{13}C and the ^{15}N spectra and to adjust the Hartman–Hahn matching condition for the cross-polarization experiments. Different numbers of transients were recorded for each compound in order to obtain an adequate signal to noise ratio.

The SPINAL64 sequence was used for heteronuclear decoupling during acquisition with a proton field H_{1H} that satisfied $\omega_{1H}/2\pi = \gamma_H H_{1H} =$ 65 kHz (Fung et al., 2000) and a recycling delay of 5 s. The assignment of the ^{13}C solid state NMR spectra for RIF was carried out by comparing the chemical shifts obtained for the solids with those in solution, taking into account the NQS experiment and the assignments presented by Przybylski et al. (2014) and Agrawal et al. (2004). In addition, the assignment of the ^{15}N solid-state NMR spectra for RIF was carried out by comparing the chemical shifts with those reported by Przybylski et al. (2014).

3.3.5. Fourier Transformed Infrared Spectroscopy (FTIR)

The infrared spectra of the samples dispersed at 1% of drug in the KBr disks were recorded on a NICOLET FTIR (360 FTIR ESP, Thermo Nicolet, Avatar, USA) spectrometer. Samples were scanned from 4000 to 400 cm^{-1}, and the recording conditions were resolution, 8.0; sample scan, 40. Data were analyzed using OMNIC software.

3.4. Preparation of Rifampicin Dihydrate (RIF·$2H_2O$)

RIF·$2H_2O$ was obtained adapting a methodology described by Henwood et al. (2001). Briefly, 1.10 g of RIF was dissolved in 50 mL of anhydrous ethanol at 60 °C. The solvent was evaporated in a Phoenix Instrument Rotavapor (Garbsen, Germany) at room temperature and the crystallized material was removed from the flask and stored under vacuum at room temperature until constant weight. The p-XRD and DSC patterns observed were in agreement with those reported previously by Son and McConville (2011) and Henwood et al. (2001).

3.5. Processing Behavior of CMC-RIF Granules

The flow properties of CMC-RIF were characterized in terms of angle of repose, bulk density, tapped density, Carr index and Hausner ratio using a method described in the European Pharmacopeia (Section 2.9.15–16).

3.6. Water Uptake

Disks (13 mm of diameter) containing powders in the amounts described in Table 1 were prepared by compression at 2 t in a hydraulic press (Delfabro, Argentina). Each disk was subjected to water uptake assays using an Enslin's apparatus as described by Nogami et al. (1969) at

Table 1
Amount of RIF or CMC powders used to make disks for water uptake assay.

Disk	mg of RIF	mg of CMC
RIF	286 ± 4	–
CMC-RIF	285 ± 6	79 ± 2
CMC + RIF	288 ± 3	80 ± 1
CMC	–	83.3 ± 0.1

a room-controlled temperature. All assays were performed in triplicate and the water uptake was expressed in mL per gram of solid.

3.7. Release of RIF From CMC-RIF Matrices

Matrices containing 300 mg of RIF were obtained by compacting 453.1 mg of CMC-RIF in a single punch tablet machine (Talleres Sanchez, CS3-GMP, Argentina). The obtained matrices presented an average hardness of (25 ± 7) 10^4 Pa ($n = 10$; AVIC, Argentina).

The release rate of RIF from the CMC-RIF matrices was measured in a rotating-basket apparatus (Hanson Research, Model SR II, USA) using the United States Pharmacopoeia (2015) dissolution method for RIF capsules (900 mL of HCl 0.1 M; 100 rpm; 37 ± 0.5 °C). In addition, the RIF released was determined by comparison with a standard solution having a known concentration of RIF in the same medium (*i.e.* 300 mg of RIF in 900 mL of HCl 0.1 M), which had been prepared concomitantly and maintained in the water bath for the same period of time (United States Pharmacopoeia (2015)).

Before each sampling time, 10 mL of medium was taken out of the vessel, filtered through a Teflon® membrane (10 μm pore size) and then returned to the vessel in order to saturate the filter (United States Pharmacopoeia (2015)). Finally, samples of 5 mL were taken at 5, 15, 30, 45, 60, 90 and 120 min and replaced with 5 mL of preheated fresh medium before being analyzed spectrophotometrically at 472 nm (UV–Vis Evolution 300 spectrophotometer, Thermo Electron Corporation, USA).

For comparison two commercially available immediate release oral dosage forms of RIF, designated Formulations (1) and (2), were subjected to the same dissolution experiments. Formulation (1) (RIFADIN®, Sanofi-Aventis Argentina SA, Argentina, hard gelatin capsules) contained 300 mg of RIF (representing an 83% w/w of the capsule content), 50 mg of corn starch and 10 mg of magnesium stearate. Formulation (2) (Rifampicina Fabra®, Fabra SA, Argentina, hard gelatin capsules) contained 300 mg of RIF (representing a 60% w/w of the capsule content), 5 mg of magnesium stearate and mannitol qs to 500 mg.

The dissolution efficiency (DE) was calculated from the RIF concentration *versus* time profiles at 5 and 15 min using the following equation:

$$DE_t = \frac{AUC_t}{AUC_{100\%}} \times 100 \quad (2)$$

where AUC_t is the area under the curve of the dissolution profile at a certain time, t, and $AUC_{100\%}$ is the rectangular area corresponding to a 100% dissolution over the same time. All experiments were run in triplicate, and the DE values were compared by a multiple pairwise ANOVA (Tukey test) at a 95% confidence interval.

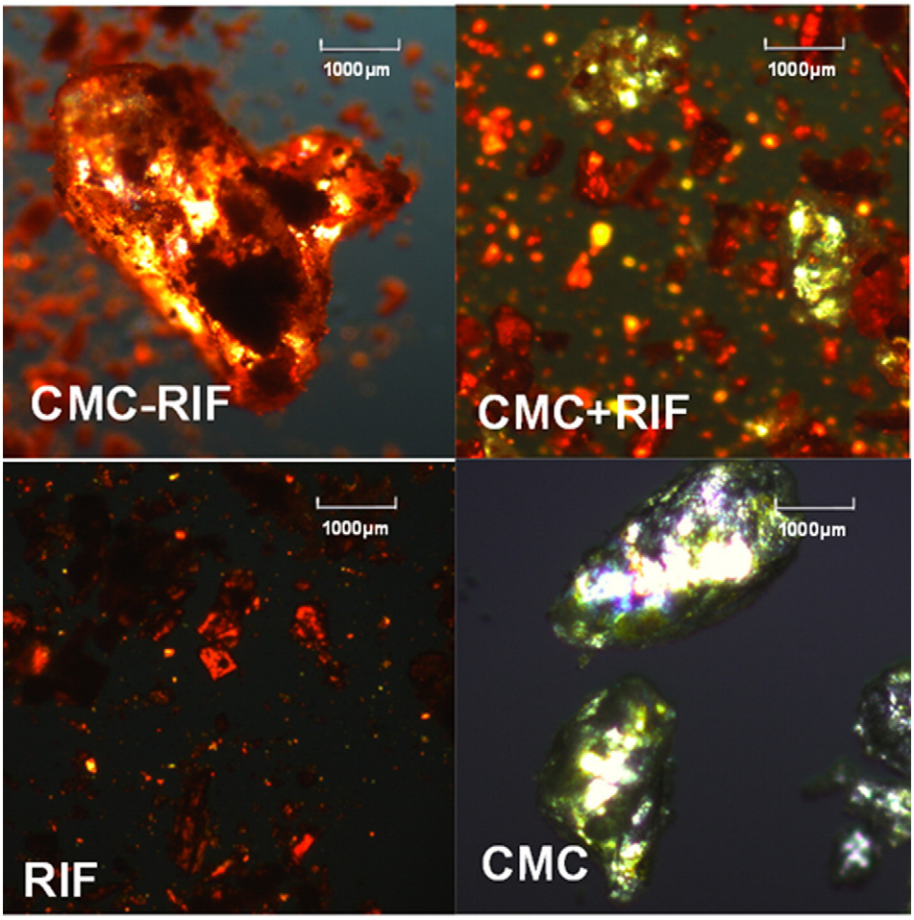

Fig. 2. Optical images (4×) of CMC-RIF, their precursors and the physical mixture obtained by polarized optical microscopy.

4. Results

4.1. Preparation of CMC-RIF

CMC-RIF was obtained by impregnation, using ethanol to promote interaction between CMC and RIF. When the materials were dried in an oven, the solvent easily evaporated. Similar results were reported by Ramírez Rigo et al. (2009) after loading CMC with atenolol and metoclopramide.

Observation of the particles under polarized light enabled the RIF crystals, which are light refringent, to be differentiated from the amorphous particles of CMC. These individual particles of CMC and RIF can be observed in the physical mixture CMC + RIF (Fig. 2), whereas in CMC-RIF, the particles of CMC are covered by RIF crystallized on the surface. Preliminary experiments comparing different CMC:RIF ratios (CMC-$RIF_{0.8}$ and CMC-$RIF_{0.6}$) showed no differences in RIF crystal morphology when observed under polarized light.

4.2. RIF Content in CMC-RIF Granules

The nitrogen content determination revealed 75.8 mg RIF per 100 mg of CMC-RIF. Notice that this value is slightly below the predicted theoretical content (78.3% w/w), suggesting that the incorporation of approximately 2.5% of water had taken place in the solid material. After dissolution in acidic media, CMC-RIF released 95.7% of the theoretical loading of RIF.

4.3. Solid-state Characterization of CMC-RIF

The solid products CMC-RIF, CMC, RIF and CMC + RIF were characterized by polarized optical microscopy, p-XRD, thermal analysis, ^{13}C and ^{15}N solid state NMR and FT-IR.

Their p-XRD profiles are shown in Fig. 3, where RIF raw material presents a diffraction pattern revealing the characteristic peaks of the crystalline form I of anhydrous RIF at 13.65 and 14.35° 2θ, as previously described by Agrawal et al. (2004) with a similar pattern being observed in the physical mixture.

CMC-RIF had a crystalline pattern completely different from that of RIF, with 2θ being similar to those previously described for RIF·$2H_2O$ (Son and McConville, 2011; Henwood et al., 2001), with only minor differences between values of 25–30 of 2θ.

Ionic interaction between drugs and polyelectrolytes is characterized by the loss of signals from the crystalline drugs (amorphization) (Ramírez-Rigo et al., 2014; Guzmán et al., 2012; Ramírez Rigo et al., 2009; Bermúdez et al., 2008). Although the p-XRD of CMC-RIF suggests that the interaction between RIF and CMC is not ionic, other kinds of interactions cannot be ruled out.

Thermograms representing weight loss and its derivative as a function of temperature are shown in Fig. 4. It can be observed from the TGA profiles that RIF did not lose weight on being heated from room temperature to 225 °C, after which a significant reduction of the mass is observed. Accordingly, the DSC thermogram (Fig. 5) did not reveal any events until the melting and exothermic degradation peak was reached at 252 °C (onset 248 °C, recovery 270 °C), which is characteristic of the crystalline form I of RIF.

For CMC, the TGA profile showed a gradual weight loss (5.0%) from room temperature to 202 °C, resulting from dehydration and a decomposition process, which in fact reached a maximum at 262 °C. The DSC thermogram of CMC revealed a wide exothermic degradation peak at 247 °C (onset 228 °C; recovery 255 °C), with the physical mixture CMC + RIF showing a behavior consistent with the sum of both components.

The TGA thermograms of both RIF·$2H_2O$ and CMC + RIF·$2H_2O$ physical mixture indicated two main events. The first one was a steep weight loss with a maximum at 137 °C, associated to the release of crystallization water that corresponded to 2 mol of water per mole of RIF

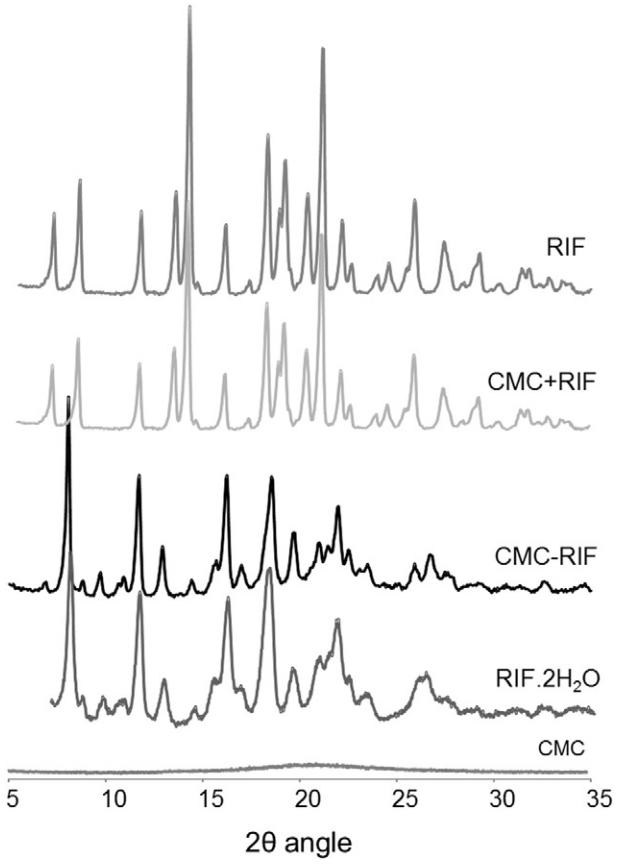

Fig. 3. Powder X-ray diffraction patterns of CMC-RIF, their precursors and the physical mixture CMC + RIF. The RIF·$2H_2O$ diffraction pattern was obtained for comparative purposes.

and the second weight loss was due to RIF decomposition with a maximum at 255 °C. In agreement, their DSC thermograms showed an endothermic event between 144 °C and 163 °C resulting from a solid-solid phase transition that overlapped dehydration, fusion and recrystallization. An exothermic degradation peak was also observed at 256 °C (Henwood et al., 2001). RIF·$2H_2O$ and CMC + RIF·$2H_2O$ physical mixture were subjected to second scan DSC to observe the transitions in the absence of the broad evaporation peak of water. As observed in Fig. 5, crystallization water was easily lost when the samples were heated 1 min at 80 °C. In line with Henwood et al. (2001) report, no fusion was observed for the anhydrous drug and the small solid-solid transition endotherm was observed at 156 °C (dashed line in Fig. 5).

CMC-RIF, in contrast, presented a thermal behavior quite different from their starting materials and physical mixtures CMC + RIF and CMC + RIF·$2H_2O$. In agreement with the RIF content value described in Section 4.2, the TGA profile of CMC-RIF revealed a gradual 2.3% reduction of weight, assigned to water loss between 30 and 161 °C. Finally, a second weight loss (with maximum at 209 °C) was ascribed to decomposition. In a similar way, the DSC thermogram of CMC-RIF indicated an almost imperceptible desorption endotherm between 43 and 170 °C and an exothermic degradation peak at 256 °C. However, unlike RIF·$2H_2O$ or the CMC + RIF·$2H_2O$ physical mixture, neither fusion nor crystalline dehydration was observed in CMC-RIF, indicating that there was an interaction between CMC and RIF.

These events observed by TGA and DSC were confirmed by HSM. In fact, dehydration in RIF·$2H_2O$ and CMC + RIF·$2H_2O$ was evidenced by an intense release of vapor bubbles from the surface of RIF crystals accompanied by a morphological change in the crystal shape that confirmed the solid-solid phase transition already observed by DSC at the same temperature (Chadha et al., 2012). In contrast, CMC-RIF had a moderate release of vapor bubbles from 52 °C, showing a behavior

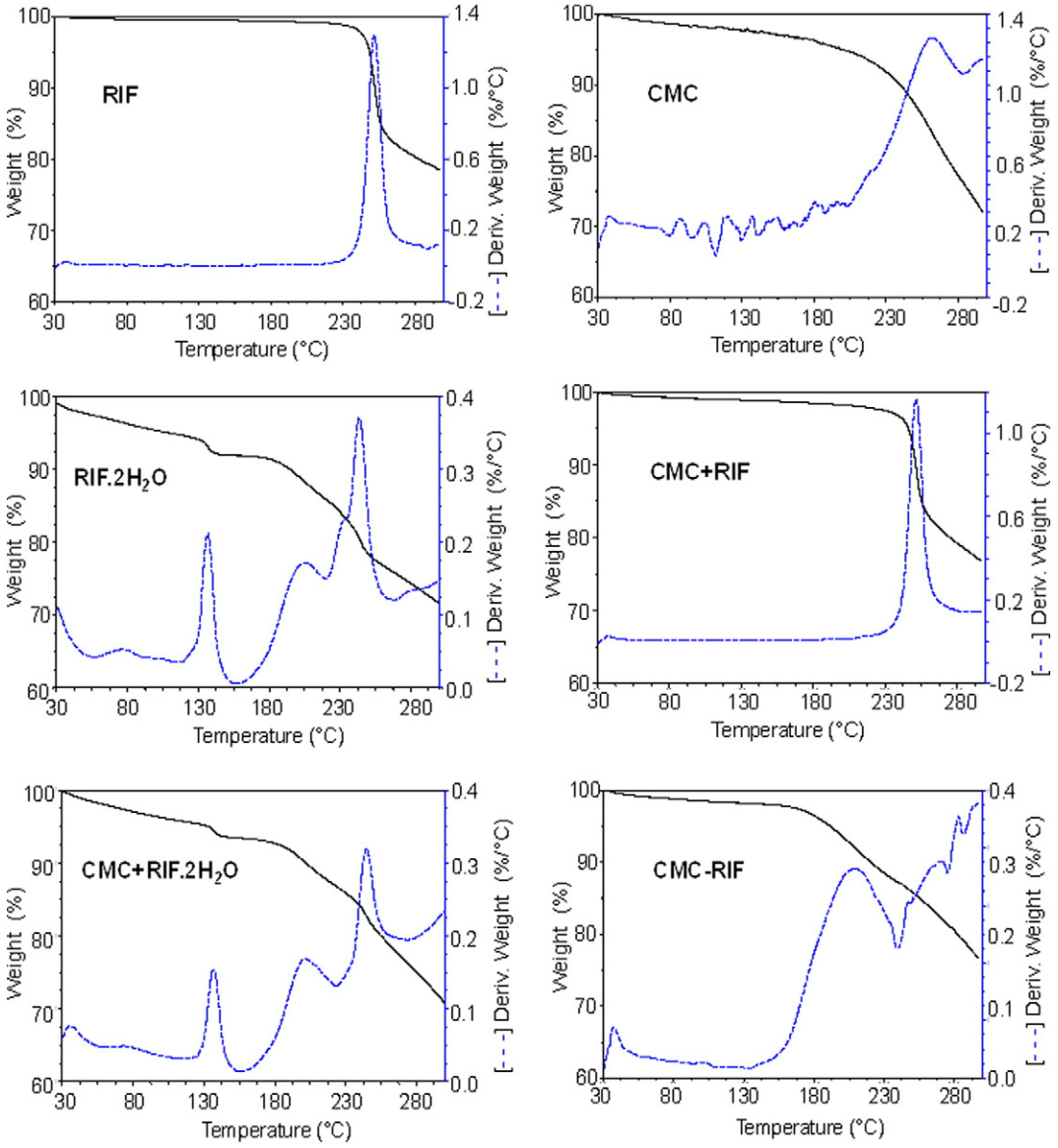

Fig. 4. TGA (solid line) and dTGA (dashed line) traces of CMC-RIF, their precursors and the physical mixtures CMC + RIF and CMC + RIF·2H_2O.

similar to that observed by DSC and TGA. Neither morphological changes nor phase transitions were observed. Finally, decomposition, revealed by darkening of the solids, was noticed for all the samples at similar temperatures to those observed in DSC and TGA.

The ^{13}C CP-MAS NMR solid-state spectra of RIF, CMC, CMC-RIF and RIF·2H_2O are shown in Fig. 6. The spectrum of CMC displayed broad signals, with this fact, together with the low proportion of CMC in CMC-RIF (only 24.18% w/w) being the reason why CMC signals cannot be clearly observed in the CMC-RIF spectrum.

The assignment of the ^{13}C NMR spectrum for RIF (Supplementary material Table S1) confirmed that it was of crystalline form I, since only one resonance was present in the high ppm region (180–200 ppm), belonging to the carbonyl at C11 (Agrawal et al., 2004).

The ^{13}C NMR spectrum of CMC-RIF presented major differences compared to RIF, as the resonances of C8 (183.8 ppm) and C11 (188.1 ppm) in CMC-RIF were shifted to higher ppm (15.2 ppm) and lower ppm (7.9 ppm), respectively, with respect to RIF. This behavior can be explained by a deprotonation process of the most acidic OH phenolic group in C8. The delocalization of the π-electron cloud causes the loss of the C(11) O ketone double bond, as can be concluded by the shift to lower frequencies of the C(11) resonance. This information suggests that RIF crystallizes as a zwitterion in CMC-RIF. Related to this, Przybylski et al. (2014) reported a zwitterionic anhydrous form of RIF, whose resonances were shifted by 15.6 ppm up-field (C8) and 11.3 ppm down-field (C11) compared with the RIF form I.

Since p-XRD of CMC-RIF showed some similarities with RIF·2H_2O, its ^{13}C NMR spectrum was also obtained. It is known that RIF·2H_2O crystallizes as a zwitterion (Henwood et al., 2001). Here, the ^{13}C NMR spectrum presented a broadening of the signals compared with CMC-RIF, indicating a lower degree of crystallinity than in CMC-RIF.

In order to obtain a better understanding of the nature of the interactions present in CMC-RIF, the ^{15}N and ^{1}H-^{15}N SCT CP-MAS spectra were taken. The spectra corresponding to RIF and CMC-RIF are shown in Fig. 7, and the chemical shifts are given in the supplementary material Table S2.

The ^{15}N CP-MAS spectrum of RIF presented the signals corresponding to the four nitrogens in the molecule at similar chemical shifts as those previously reported by Przybylski et al. (2014) for RIF form I. In addition, the chemical shifts observed in ^{15}N CP-MAS spectrum of CMC-RIF were qualitatively similar to those reported for the zwitterionic form of RIF. In fact, the signal corresponding to N15 in the CMC-RIF spectrum was shifted to lower ppm and overlapped the signal

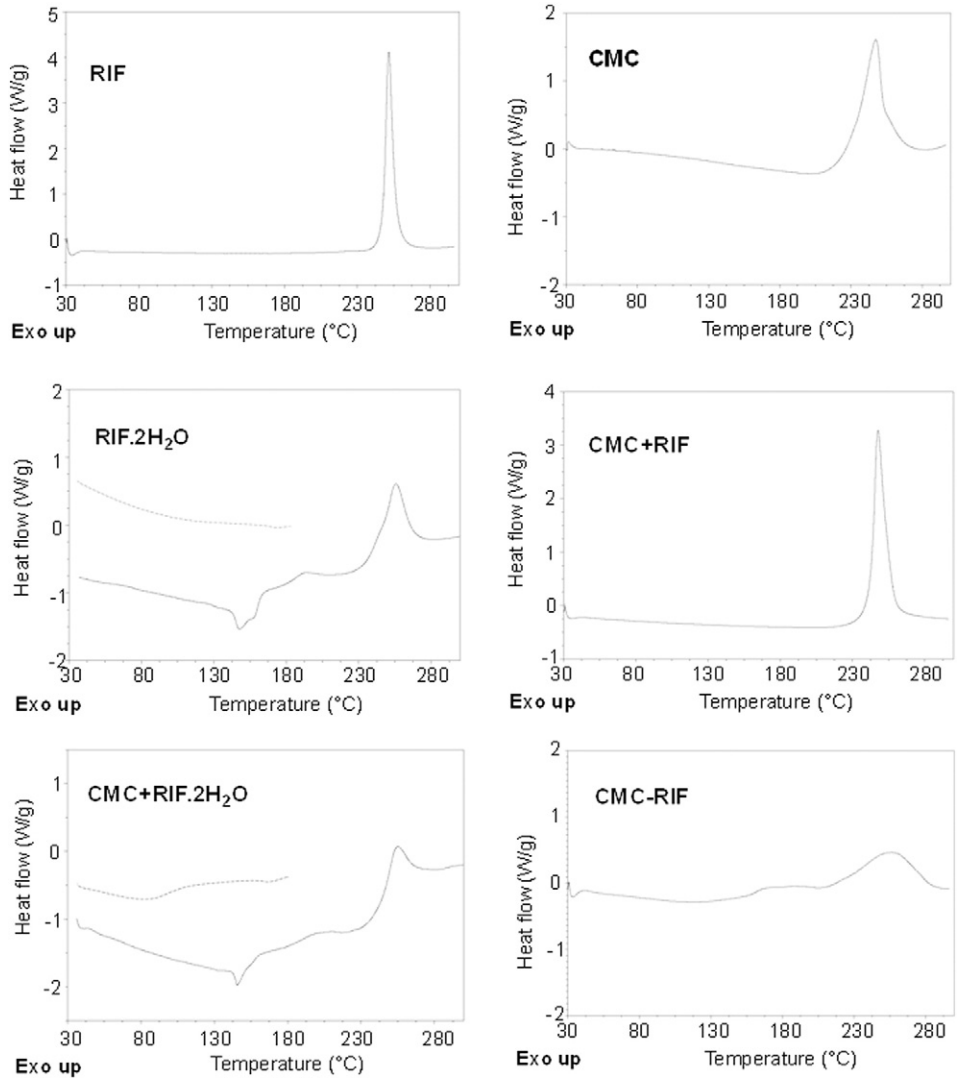

Fig. 5. DSC traces of CMC-RIF, their precursors and the physical mixtures CMC + RIF and CMC + RIF·$2H_2O$. The grey dashed lines in RIF·$2H_2O$ and CMC + RIF·$2H_2O$ physical mixture show the second scan DSC of these samples.

corresponding to N39, which was also slightly shifted to a lower ppm with respect to its resonance in RIF. Moreover, the resonance of N38 was moved to higher frequencies compared to that of RIF. However, as the changes in N15 and N38 were more intense in CMC-RIF than those informed for the already mentioned zwitterionic form of RIF (13 and 9 ppm, respectively), this suggests that they may be involved in some interactions with CMC.

The ^{15}N CP-MAS spectrum of RIF·$2H_2O$ revealed no signals, although this was obtained under the same conditions, which might have been a result of the widening of the signals due to a lower crystallinity degree in ^{13}C NMR.

In the ^{1}H-^{15}N SCT CP-MAS spectrum for RIF (Fig. 7), only the N15 signal can be observed, since it is the only nitrogen directly bonded to a hydrogen atom. However, two signals belonging to N15 and N43 can be seen in CMC-RIF, supporting the assumption that RIF crystallized in a zwitterionic form in CMC-RIF.

The FTIR spectra also showed significant changes among RIF, CMC-RIF, RIF·$2H_2O$ and the physical mixtures (Fig. 8A and B). The absorption bands that characterize RIF form I, according to Agrawal et al. (2004), are found at 3493 cm^{-1} (ansa O—H), 1725 cm^{-1} (carbonyl C35═O), 1645 cm^{-1} (furanone C11═O) and 1565 cm^{-1} (C═O amide). Here, the perturbed C—H Bohlmann bands for the N—CH_3 group appeared at 2801 cm^{-1} in RIF (Fig. 8A) (Przybylski et al., 2014), with the physical mixture CMC + RIF presenting a similar profile to that of RIF.

In agreement with its zwitterionic nature, RIF·$2H_2O$ revealed no Bohlmann bands. In addition, the wide band ascribed to the naphthalene group presented a hypsochromic shift from 1548 cm^{-1} in RIF to 1560 cm^{-1} in RIF·$2H_2O$, which is consistent with the resonance of the O8 phenolate ion in the naphthalene ring (Fig. 8B). In the FTIR spectrum of CMC-RIF, the Bohlmann bands were absent and the bands ascribed to the naphthalene group were observed at 1564 cm^{-1}, thus confirming the zwitterionic nature of RIF in CMC-RIF.

4.4. Water Uptake

Water sorption was evaluated to assess the hydrophilicity of the solids using the Enslin's apparatus, which allows the volume of liquid captured by capillarity at pre-established time intervals to be measured. Fig. 9 shows the water uptake of the solids (mL/g of solid) at room temperature as a function of time (min). The uptake of water in CMC was very fast, reaching a plateau after incorporation of 150% its initial weight in water in less than a minute. As expected, RIF absorbed an almost imperceptible amount of water, whereas in the case of CMC-RIF, the plateau was reached 10 min after incorporation of 100% its initial weight

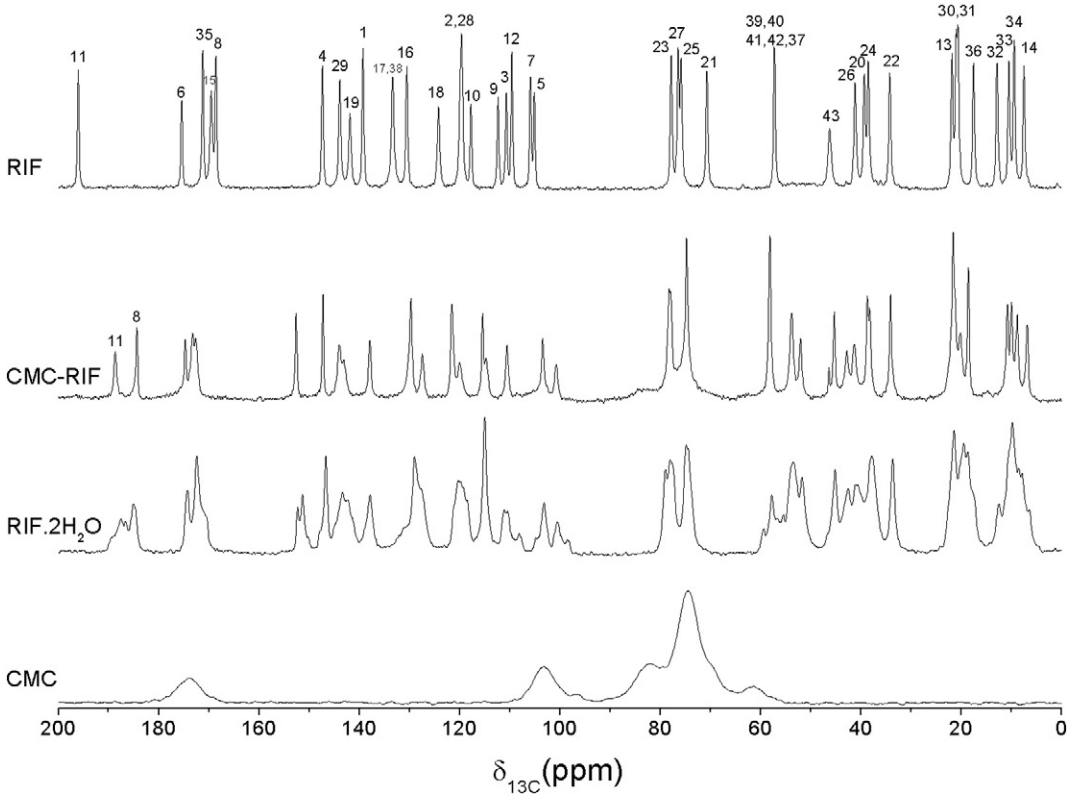

Fig. 6. ^{13}C CP-MAS NMR solid-state spectra of RIF, CMC-RIF, RIF·$2H_2O$ and CMC.

in water, thereby improving the hydrophilicity of RIF. In a similar way, the physical mixture CMC + RIF incorporated 90% its weight in water after 3 min. No evidence of the development of a hydrogel layer that could delay drug delivery was observed in either case, which is desirable for the fast release of RIF.

4.5. Processing Behavior of CMC-RIF and Drug Release

Table 2 shows the rheological properties of RIF and CMC-RIF, with CMC-RIF demonstrating flow properties significantly improved with respect to those of RIF, which are adequate for the production of solid

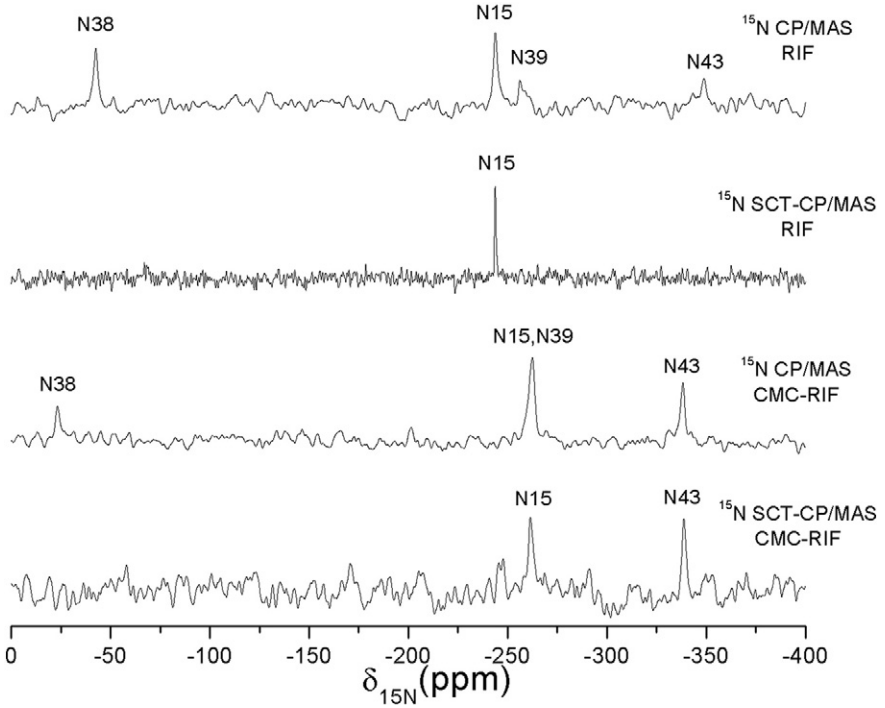

Fig. 7. ^{15}N and ^{1}H–^{15}N SCT CP-MAS solid-state NMR spectra of RIF and CMC-RIF.

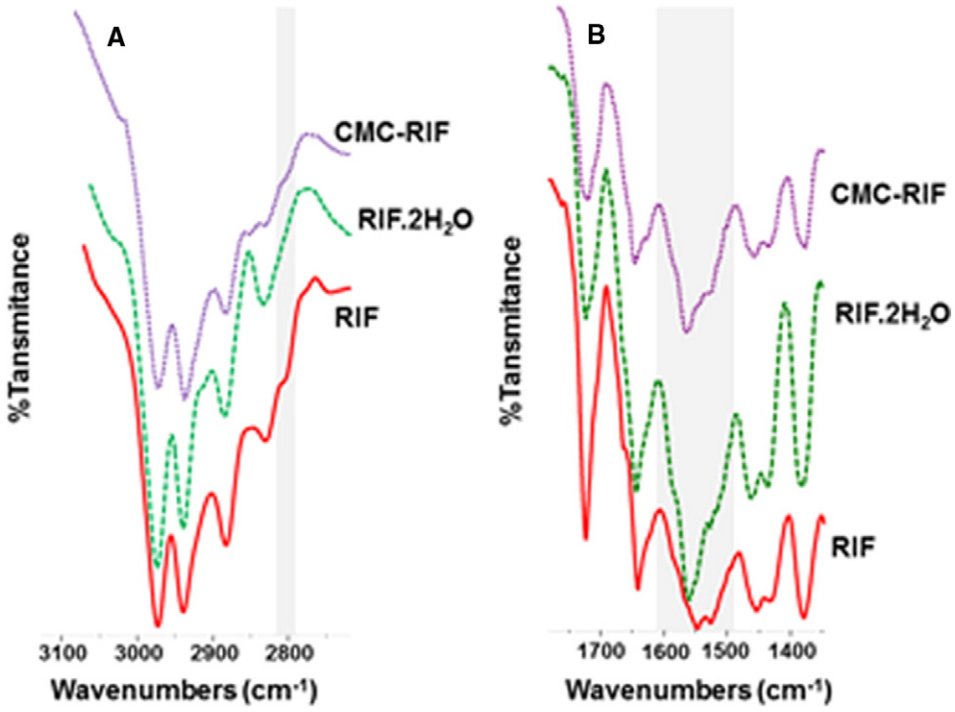

Fig. 8. Representative FTIR spectra of: RIF, RIF·$2H_2O$ and CMC-RIF. The zwitterionic nature of RIF in CMC-RIF is confirmed by the absence of the band corresponding to stretching of the non-protonated N—CH_3 group (2801 cm^{-1}) and the hypochromic shift of the band ascribed to the naphthalene group at 1564 cm^{-1}.

dosage forms. In fact, according to European Pharmacopeia scores, the angle of repose of CMC-RIF changed from poor to excellent, its Hausner ratio changed from poor to fair and the Carr Index from poor to passable.

Fig. 10A shows that CMC-RIF matrix exhibited a complete disintegration into individual swollen particles in an acidic medium, resulting in a very fast release of RIF ((99 ± 3)% at 15 min). For comparison, the dissolution profiles of two commercially available oral solid dosage forms are also shown in Fig. 10A, where it can be observed that the DE of RIF was significantly higher in CMC-RIF matrices compared with Formulations (1) and (2) (Fig. 10B, $p^{\sim}0.05$).

5. Discussion

Traditional polyelectrolyte-drug complexes are usually obtained by mixing a polyelectrolyte with an oppositely charged drug in a convenient medium (water or ethanol) able to dissolve one or both components (Guzmán et al., 2012; Ramírez Rigo et al., 2009). The resulting solid materials are amorphous molecular dispersions of the drug ionically bonded to the polymeric carrier. In contrast, CMC-RIF is a crystalline material with sharp peaks observed by p-XRD. No evidence of acid-base reaction between the acidic groups of CMC and the amine groups of RIF was found in CMC-RIF, in which CMC particles are covered by zwitterionic RIF. Therefore, CMC-RIF is a crystalline solid dispersion rather than the commonly designated amorphous one, since RIF crystals coexist with CMC particles. The p-RXD profiles of CMC-$RIF_{0.8}$ and CMC-$RIF_{0.6}$ presented sharp peaks at the same 2 θ angles than CMC-RIF suggesting that such crystalline dispersions can be obtained using other CMC:RIF ratios (Supplementary material Fig. S1). Considering that CMC-RIF allows a higher loading capacity, this was selected to complete the studies.

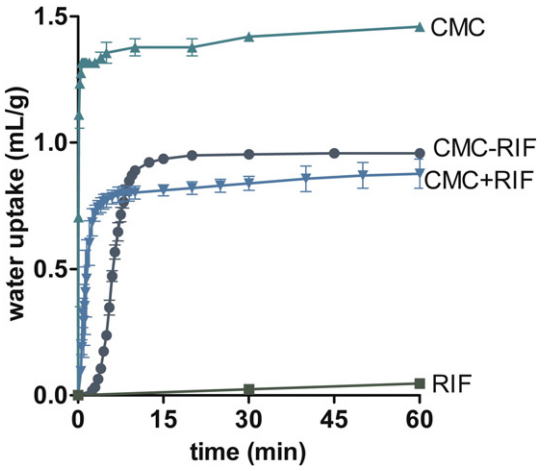

Fig. 9. Water uptake (mL) per gram of solid in disks of CMC-RIF, RIF, CMC, and the physical mixture CMC + RIF as a function of time. The amount of CMC is the same in all systems. The CMC content in CMC-RIF improves significantly the hydrophilicity of RIF.

CMC was selected as a carrier since CMC-complexes have previously shown a very rapid release of some basic drugs in acidic media (Ramírez Rigo et al., 2009). Protonated CMC is insoluble in water and other pharmaceutical solvents. RIF is insoluble and unstable in water but is slightly soluble in ethanol (United States Pharmacopoeia (2015)) which was selected as the interaction medium. Unlike the conventional polyelectrolyte-drug complexes, only a fraction of RIF is dissolved in ethanol during CMC-RIF preparation.

Exhaustive characterization using ^{13}C and ^{15}N NMR spectra and FTIR confirmed that no ionic interaction occurred between RIF and CMC. However, differences observed in the thermal analysis indicated that some other non-covalent interactions were taking place. From the ^{13}C and ^{15}N NMR spectra, we can conclude that, in CMC-RIF, RIF is crystallized in a zwitterionic form that interacts with the surface of CMC particles. This was confirmed by the ^{1}H-^{15}N SCT CP-MAS and the FTIR spectra

Table 2
Rheological properties of RIF and CMC-RIF.

Sample	Angle of repose	Bulk density	Tap density	Carr's index	Hausner's ratio
RIF	48 ± 3	0.51 ± 0.01	0.69 ± 0.01	26.0 ± 0.5	1.35 ± 0.01
CMC-RIF	22 ± 1	0.36 ± 0.01	0.44 ± 0.01	21.0 ± 2.0	1.20 ± 0.04

reinforce these results. It is worth noting that the RIF form I used as the starting material was completely transformed into highly ordered zwitterionic crystals, which was the only crystalline phase present in CMC-RIF.

It is known that in protic solvents (such as ethanol), the proton of the OH phenolic group is transferred to the N43 atom to form the zwitterionic species, which prevails in solution (Pyta et al., 2012). Thus, the crystalline reorganization may have been due to the existence of a hydrogen bonding interaction between the dissolved fraction of RIF and the carboxylic acid groups in the surface of CMC particles during CMC-RIF preparation, which led to a preferential orientation of RIF zwitterionic molecules and favored the formation of the zwitterionic RIF nucleus on CMC particles. Thus, the remaining RIF might have crystallized as a zwitterion when the ethanol used in the preparation of CMC-RIF evaporated (Fig. 11). The induction of preferential orientations of crystalline solids in the presence of polymers has been previously described (Curcio et al., 2014; Pfund et al., 2015). Although an acid-base interaction between the carboxylic acid groups in the surface of CMC and the amine groups of non-zwitterionic RIF molecules in solution cannot be ruled out, it does not result in formation of crystalline nuclei since zwitterionic RIF is the only crystalline phase present in the solid.

Notice that the interaction between RIF and CMC seemed to occur only on the surface of CMC and therefore, the ratio of carboxylic equivalents in CMC:amine groups of RIF is not an important aspect. In fact, p-XRD of CMC-$RIF_{0.8}$ and CMC-$RIF_{0.6}$ showed the same crystalline profile than CMC-RIF. However, more studies are required to confirm this hypothesis at ratios different from the ones used in our study.

It is widely known that RIF has a poor hydrophilic behavior (Henwood et al., 2001), which could strongly affect the dissolution processes. A noticeable difference could be observed in the water uptake of CMC-RIF compared to pure RIF. This behavior could possibly be due to the RIF crystals attached to the surface of CMC forming a single particulate material, where the high hydration capacity of CMC improved the wetting of RIF. Such a system is similar to the solid dispersions obtained by a surface-attached methodology in which a hydrophilic carrier was attached to the drug, thus increasing its wettability (Joe et al., 2010; Li et al., 2010; Park et al., 2009; Yan et al., 2012). In fact, Ramírez Rigo et al. (2009) reported that, in matrices containing CMC, water diffuses quickly through the matrix pores and completely wets them. The uptake of water in CMC-RIF was higher than that of the physical mixture. This difference may have been related to the crystallization of RIF as a zwitterion, which consequently contributed to the hydrophilicity of the system. In addition, the slower uptake rate observed in CMC-RIF during the first 5 min is probably associated with the fact that CMC was covered by RIF crystals (major component), which can partially occlude some the pores of the matrix and therefore produce a delay in water entry.

The CMC-RIF matrices released RIF at a very fast rate, with both the release rate and DE of RIF being significantly higher than that observed for the available commercial formulations. Such behavior can be due to both the high hydration capacity of CMC and the zwitterionic form of RIF. As previously reported, the zwitterionic species of a drug is more hydrophilic and is also more soluble than its non-zwitterionic counterpart (Olivera et al., 2003).

The fast dissolving performance of CMC-RIF matrices is able to deliver a major extent of RIF in the absorption site, which is highly desirable for the improvement of RIF bioavailability (Agrawal and Panchagnula, 2004).

It was reported that a reduction of 10% of the dose of RIF can contribute towards development of drug resistance (Sankar et al., 2003). In fact, sub-therapeutic plasma levels of RIF could increase the risk of resistance taking into account that its activity is highly dose-dependent and the RIF resistance mechanism develops in only one step (Ellard and Fourie, 1999; Jindani et al., 1980; Telenti et al., 1993). In this context, Agrawal and Panchagnula (2004) observed that in some commercial formulations only 80% of the labeled dose of RIF dissolved in 45 min due to its interaction with some acidic excipients. Our results show that the interaction between RIF and CMC is reversible, allowing the complete release of RIF from the CMC-RIF matrices.

The very fast dissolution rate observed may result in a better absorption of RIF, since it is a BCS class 2 drug (Becker et al., 2009). Hence, CMC-RIF matrices would assure a fast and complete availability of the drug in the absorption site and could help to maintain therapeutic levels of RIF. *In vivo* studies are currently been carried out in our lab to try to confirm this.

One of the major underlying problems for RIF is the fact that acidity is required for dissolution of the current formulations. The chemical instability of RIF is also well known, which is favored in the acidic environment of the stomach (Sankar et al., 2003). In addition, RIF has a pH-dependent solubility, which shows a minimum at pHs between 3 and 8 (Panchagnula et al., 2007). In consequence, dissolution of RIF will depend on stomach acidity, and situations in which the stomach pH increases (food effects, co-administration of proton pump inhibitors, illness, age) will have a negative impact on its dissolution rate and bioavailability, in unpredictable and uncontrolled ways (Clinical Pharmacology, 2016). In this context, the very fast dissolution observed with CMC-RIF could help to reduce not only RIF instability but also the impact of such factors by providing a short residence time in the stomach.

Although several authors have reported systems to improve the performance of RIF-containing formulations (Wang et al., 2013; Gohel and Sarvaiya, 2007; Singh et al., 2014; Prabakaran et al., 2004; Pund et al., 2011), only a few have attempted to increase the dissolution rate of RIF and none of these investigations resulted in an enhanced

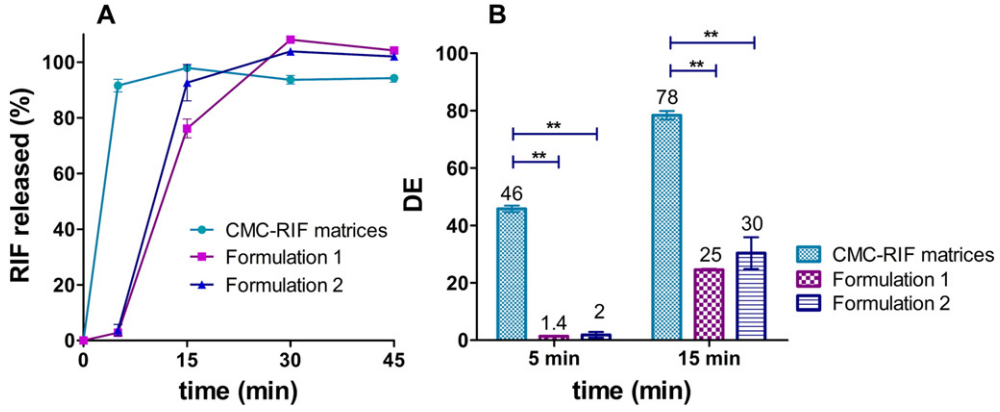

Fig. 10. A. Release profile of RIF in HCl 0.1 M from CMC-RIF matrices, Formulations (1) and (2). B. Dissolution efficiency (DE) at 5 and 15 min in HCl0.1 M. Results are expressed as mean ± SEM.

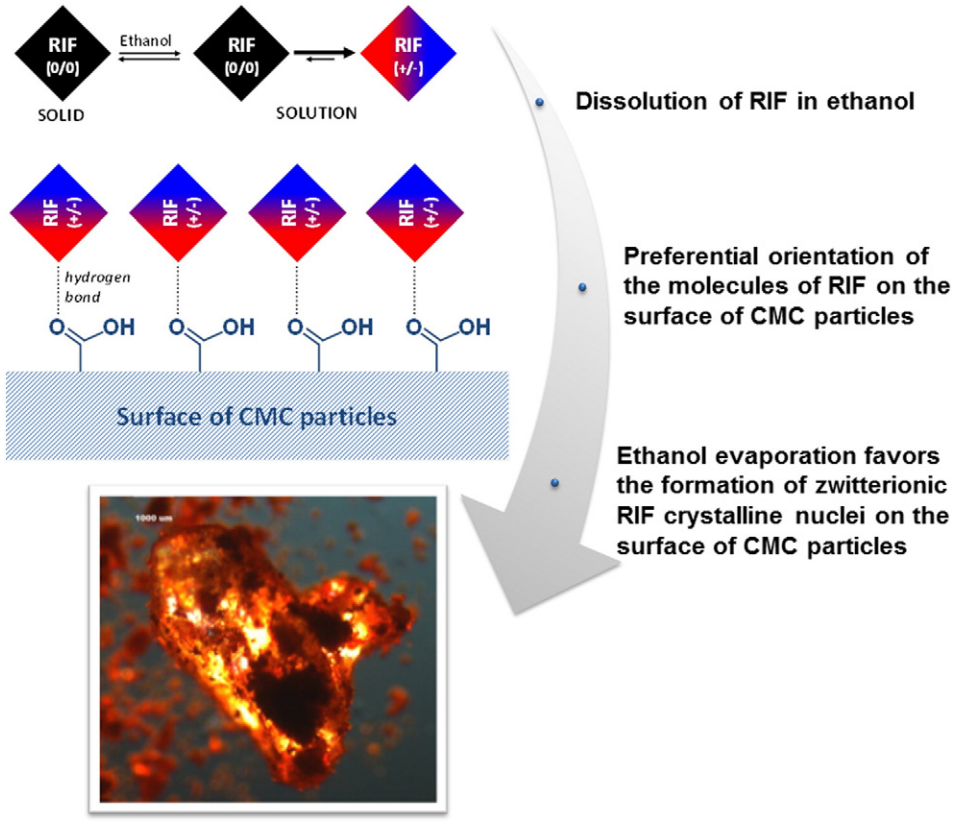

Fig. 11. Proposed mechanism for the formation of CMC-RIF crystalline solid dispersion.

performance such as the CMC-RIF matrices reported here. For instance, Yadav et al. (2009) obtained granules of RIF using polyethylene glycol and poloxamer as a melt binder, which improved the dissolution rate of RIF to 80% in 15 min in HCl 0.1 N. In another study, Schianti et al. (2013) obtained nanoparticles of RIF that improved the release of RIF with respect to the raw material from 60 to 80% when dissolved at 45 min in a buffer solution with pH of 7.4.

Hydrolysis of RIF in the acidic environment of the stomach is accelerated by the presence of isoniazid in a magnitude proportional to isoniazid concentration (Shishoo et al., 1999; Singh et al., 2000). Since both drugs are usually formulated in a fixed drug combination, the development of formulations that allow segregated delivery of RIF and isoniazid has been previously proposed to improve RIF bioavailability. Related to this, Silva et al. (2014) formulated bilayer tablets having an immediate release layer of RIF associated to an isoniazid-retarded layer. However, the percentage of the different RIF layers dissolved in 30 min in gastric simulated fluid was variable (between 65.7 and 93.4%) and incomplete, which was attributed to polymorphic transitions of the drug.

The good flow properties of CMC-RIF are adequate for producing tablets by the direct compression method. Thus, the formulation of tablets from CMC-RIF can be a simple, cost-effective and versatile production method. In addition, CMC-RIF can be useful to develop fixed dose combination oral systems to attain segregated delivery of RIF and isoniazid.

In view of the fact that TB is a disease strongly associated to poverty, there is a high incidence in underdeveloped and developing countries. Thus, it is essential that the delivery systems developed have an acceptable cost-benefit ratio so that the product is widely available to the public health systems of these countries (Goldberg, 2010). CMC is included in several pharmacopeias (Argentinian Pharmacopeia, Japanese Pharmacopeia) and its sodium salt is listed by the FDA as a Generally Recognized as Safe (GRAS) compound (U.S. Goverment Publishing Office, 2016).

6. Conclusions

CMC-RIF is a crystalline solid dispersion that can be prepared using components and methodologies which are accessible to the health care systems of communities with limited resources. The structure-property relationships that underlie its fast dissolution behavior have been explored and the results show that CMC-RIF has significant merit and can be useful for the formulation of solid dosage forms, either alone or in combination with other antitubercular drugs. This could be a step in the right direction in addressing issues of unacceptable RIF bioavailability.

Acknowledgements

The authors wish to acknowledge the assistance of the Consejo Nacional de Investigaciones Científicas y Técnicas (CONICET, N° 11220090100761), the Comisión Nacional Salud Investiga-Ministerio de Salud de la Nación (subsidy CONV09/INST-259 and CONV10/INST-10-00046) and the Universidad Nacional de Córdoba SECYT-UNC (Argentina, subsidy Res N°: 162/12), all of which provided support and facilities for this investigation.

The authors thank to Dr. R. Carbonio from Instituto de investigaciones en físicoquimica de Córdoba (INFIQC) for the powder X-ray diffraction measurements, Dr. S. Pesce of CEQUIMAP (FCQ-UNC) for the total nitrogen assay experiment, Dr. M. Frías, Dr. G. Roca and Dr. M. Tappia of the Programa Nacional de Control de la Tuberculosis for the provision of conventional RIF formulations, Dr. C.B. Romañuk for her help in the dissolution assays and Dr. G. Barrera from Instituto de Ciencia y Tecnología de Alimentos Córdoba (ICYTAC) for the

differential scanning calorimetry measurements. Laura Carolina Luciani-Giacobbe thanks for the CONICET fellowship.

Appendix A. Supplementary data

Supplementary data to this article can be found online at http://dx.doi.org/10.1016/j.ejps.2016.10.013.

References

Agrawal, S., Panchagnula, R., 2004. Dissolution test as a surrogate for quality evaluation of rifampicin containing fixed dose combination formulations. Int. J. Pharm. 287 (1–2), 97–112. http://dx.doi.org/10.1016/j.ijpharm.2004.09.005.

Agrawal, S., Ashokraj, Y., Bharatam, P.V., Pillai, O., Panchagnula, R., 2004. Solid-state characterization of rifampicin samples and its biopharmaceutic relevance. Eur. J. Pharm. Sci. 22 (2–3), 127–144. http://dx.doi.org/10.1016/j.ejps.2004.02.011.

AOAC Official Method 991.20, 2005. Nitrogen (total) in milk. Official methods of analysis of AOAC international. In: Horwitz (Ed.), AOAC International. 18° ed., Maryland, EE.UU.

Becker, C., Dressman, J.B., Junginger, H.E., Kopp, S., Midha, K.K., Shah, V.P., Stavchansky, S., Barends, D.M., 2009. Biowaiver monographs for immediate release solid oral dosage forms: rifampicin. J. Pharm. Sci. 98 (7), 2252–2267. http://dx.doi.org/10.1002/jps.21624.

Bermúdez, J.M., Jimenez-Kairuz, A.F., Olivera, M.E., Allemandi, D.a., Manzo, R.H., 2008. A ciprofloxacin extended release tablet based on swellable drug polyelectrolyte matrices. AAPS PharmSciTech 9 (3), 924–930. http://dx.doi.org/10.1208/s12249-008-9098-9.

Chadha, R., Arora, P., Bhandari, S., Bala, M., 2012. Thermomicroscopy and its pharmaceuticals applications. Current Microscopy Contributions to Advances in Science and Technology 1013–1024.

Curcio, E., López-Mejías, V., Di Profio, G., Fontananova, E., Drioli, E., Trout, B.L., Myerson, A.S., 2014. Regulating nucleation kinetics through molecular interactions at the polymer-solute interface. Cryst. Growth Des. 14 (2), 678–686. http://dx.doi.org/10.1021/cg4015543.

Ellard, G.A., Fourie, P.B., 1999. Rifampicin bioavailability: a review of its pharmacology and the chemotherapeutic necessity for ensuring optimal absorption. International Journal of Tuberculosis and Lung Diseases 3 (11 Suppl. 3), S301–8 (discussion S317–21) http://pubget.com/paper/10593709/rifampicin-bioavailability-a-review-of-its-pharmacology-and-the-chemotherapeutic-necessity-for-ensuring-optimal-absorption\nhttp://www.ncbi.nlm.nih.gov/pubmed/10593709.

European Pharmacopoeia 8th edition, 2013. European Directorate for the Quality of Medicines & HealthCare. Council of Europe 7 allée Kastner, CS, p. 30026.

Fung, B.M., Khitrin, A.K., Ermolaev, K., 2000. An improved broadband decoupling sequence for liquid crystals and solids. J. Magn. Reson. 142 (1), 97–101. http://dx.doi.org/10.1006/jmre.1999.1896.

Gohel, M., Sarvaiya, K., 2007. A novel solid dosage form of rifampicin and isoniazid with improved functionality. AAPS PharmSciTech 8 (3), E68. http://dx.doi.org/10.1208/pt0803068.

Goldberg, A., 2010. Sociocultural factors in the health care process of patients with tuberculosis, of Vaccarezza Institute of Muñiz Hospital, 2009. Revista Argentina de Salud Pública 1 (5), 13–21.

Guzmán, M.L., Manzo, R.H., Olivera, M.E., 2012. Eudragit E100 as a drug carrier: the remarkable affinity of phosphate Ester for dimethylamine. Mol. Pharm. 9 (9), 2424–2433. http://dx.doi.org/10.1021/mp300282f.

Harris, R.K., 1994. Nuclear Magnetic Resonance Spectroscopy. Longman Scientific and Technical, London, UK.

Henwood, S.Q., Liebenberg, W., Tiedt, L.R., De Villiers, M.M., 2001. Characterization of the solubility and dissolution properties of several new rifampicin polymorphs, solvates and hydrates. Drug Dev. Ind. Pharm. 27 (10), 1017–1030. http://dx.doi.org/10.1081/DDC-100108364.

Jindani, A., Aber, V.R., Edwards, E.A., Mitchison, D.A., 1980. The early bactericidal activity of drugs in patients with pulmonary tuberculosis. Am. Rev. Respir. Dis. 121 (6), 939–949 (http://www.ncbi.nlm.nih.gov/pubmed/6774638).

Joe, J.H., Lee, W.M., Park, Y.J., Joe, K.H., Dong Hoon, O., Seo, Y.G., Woo, J.S., Yong, C.S., Choi, H.G., 2010. Effect of the solid-dispersion method on the solubility and crystalline property of tacrolimus. Int. J. Pharm. 395 (1–2), 161–166. http://dx.doi.org/10.1016/j.ijpharm.2010.05.023.

Li, D.X., Jang, K.-Y., Kang, W., Bae, K., Lee, M.H., Yu-Kyoung, O., Jee, J.-P., et al., 2010. Enhanced solubility and bioavailability of sibutramine base by solid dispersion system with aqueous medium. Biol. Pharm. Bull. 33 (2), 279–284. http://dx.doi.org/10.1248/bpb.33.279.

Ma, Zhenkun, Christian Lienhardt, Helen Mcllleron, Andrew J. Nunn, and Xiexiu Wang. 2010. "Global tuberculosis drug development pipeline: the need and the reality." Lancet 375 (9731). Elsevier Ltd.: 2100–2109. http://dx.doi.org/10.1016/S0140-6736(10)60359-9.

Mariappan, T.T., Singh, S., 2003. Regional gastrointestinal permeability of rifampicin and isoniazid (alone and their combination) in the rat. International Journal of Tuberculosis and Lung Disease 7 (8), 797–803.

Ministerio de salud, Secretaría de Políticas, Regulación e Institutos, Administración Nacional de Medicamentos, Alimentos y Tecnología Médica e Instituto Nacional de Medicamentos, 2003e. Farmacopea Argentina. [Internet]. 7° ed. Comisión Permanente de la Farmacopea Argentina, Ciudad Autónoma de Buenos Aires. http://www.anmat.gov.ar/webanmat/fna/fna_pdfs.asp.

Nogami, H., Nagai, T., Fukuoka, E., Sonobe, T., 1969. Desintegration of the aspirin tablets containing potato starch and microcrystalline cellulose in various concentrations. Chem. Pharm. Bull. 17, 1450–1455.

Olivera, M.E., Rigo, M.V.R., Chattah, A.K., Levstein, P.R., Baschini, M., Manzo, R.H., 2003. Solution and solid state properties of a set of procaine and procainamide derivatives. Eur. J. Pharm. Sci. 18 (5), 337–348. http://dx.doi.org/10.1016/S0928-0987(03)00036-8.

Panchagnula, R., Gulati, I., Varma, M.V.S., Raj, Y.A., 2007. Dissolution methodology for evaluation of rifampicin-containing fixed-dose combinations using biopharmaceutic classification system based approach. Clin. Res. Regul. Aff. 24 (2–4), 61–76. http://dx.doi.org/10.1080/10601330701683305.

Pandey, Rajesh, and Zahoor Ahmad. 2011. "Nanomedicine and experimental tuberculosis: facts, flaws, and future." Nanomedicine: Nanotechnology, Biology, and Medicine 7 (3). Elsevier Inc.: 259–272. http://dx.doi.org/10.1016/j.nano.2011.01.009.

Park, Y.J., Ryu, D.S., Li, D.X., Quan, Q.Z., Dong Hoon, O., Kim, J.O., Seo, Y.G., et al., 2009. Physicochemical characterization of tacrolimus-loaded solid dispersion with sodium carboxylmethyl cellulose and sodium lauryl sulfate. Arch. Pharm. Res. 32 (6), 893–898. http://dx.doi.org/10.1007/s12272-009-1611-5.

Pfund, L.Y., Price, C.P., Frick, J.J., Matzger, A.J., 2015. Controlling pharmaceutical crystallization with designed polymeric Heteronuclei. J. Am. Chem. Soc. 137 (2), 871–875. http://dx.doi.org/10.1021/ja511106j.

Clinical Pharmacology, 2016. Rifampin. Available in the website: <http://clinicalpharmacology.com>. (Access date: 22/07/2016).

Prabakaran, D., Paramjit, S., Jaganathan, K.S., Vyas, S.P., 2004. Osmotically regulated asymmetric capsular systems for simultaneous sustained delivery of anti-tubercular drugs. J. Control. Release 95 (2), 239–248. http://dx.doi.org/10.1016/j.jconrel.2003.11.013.

Przybylski, P., Pyta, K., Klich, K., Schilf, W., Kamieñskib, B., 2014. 13C and 15N CP/MAS, 1H-15N SCT CP/MAS and FTIR spectroscopy as tools for qualitative detection of the presence of zwitterionic and nonionic forms of ansa-macrolide 3-formylrifamycin SV and its derivatives in solid state. Magn. Reson. Chem. 52 (1–2), 10–21. http://dx.doi.org/10.1002/mrc.4028.

Pund, Swati, Amita Joshi, Kamala Vasu, Manish Nivsarkar, and Chamanlal Shishoo. 2011. "Gastroretentive delivery of rifampicin: in vitro mucoadhesion and in vivo gamma scintigraphy." Int. J. Pharm. 411 (1–2). Elsevier B.V.: 106–112. http://dx.doi.org/10.1016/j.ijpharm.2011.03.048.

Pyta, K., Przybylski, P., Wicher, B., Gdanieca, M., Stefańska, J., 2012. Intramolecular proton transfer impact on antibacterial properties of ansamycin antibiotic rifampicin and its new amino analogues. Org. Biomol. Chem. 10, 2385–2388. http://dx.doi.org/10.1039/c2ob00008c.

Ramírez Rigo, M.V., Allemandi, D.A., Manzo, R.H., 2004. A linear free energy relationship treatment of the affinity between carboxymethylcellulose and basic drugs. Mol. Pharm. 1 (5), 383–386.

Ramírez Rigo, M.V., Allemandi, D.A., Manzo, R.H., 2009. Swellable drug-polyelectrolyte matrices of drug-carboxymethylcellulose complexes. Characterization and delivery properties. Drug Delivery 16 (2), 108–115. http://dx.doi.org/10.1080/10717540802605848.

Ramírez-Rigo, M.V., Olivera, M.E., Rubio, M., Manzo, R.H., 2014. Enhanced intestinal permeability and oral bioavailability of enalapril maleate upon complexation with the cationic polymethacrylate eudragit E100. Eur. J. Pharm. Sci. 55 (1), 1–11. http://dx.doi.org/10.1016/j.ejps.2014.01.001.

Sankar, R., Sharda, N., Singh, S., 2003. Behavior of decomposition of rifampicin in the presence of isoniazid in the pH range 1–3. Drug Dev. Ind. Pharm. 29 (7), 733. http://dx.doi.org/10.1081/DDC-120021772.

Schianti, J.N., Cerize, N.N.P., de Oliveira, A.M., Derenzo, S., Seabra, A.C., Góngora-Rubio, M.R., 2013. Rifampicin nanoprecipitation using flow focusing microfluidic device. Journal of Nanomedicine & Nanotechnology 04 (04), 4–9. http://dx.doi.org/10.4172/2157-7439.1000172.

Shishoo, C.J., Shah, S.a., Rathod, I.S., Savale, S.S., Kotecha, J.S., Shah, P.B., 1999. Stability of rifampicin in dissolution medium in presence of isoniazid. Int. J. Pharm. 190 (1), 109–123. http://dx.doi.org/10.1016/S0378-5173(99)00286-0.

Silva, A., Abrahim-Vieira, B., do Carmo, F.A., do Amaral, L.H., Silva, L.C., Escudini, C.S., Lopes, M.A., et al., 2014. Segregated delivery of rifampicin and isoniazid from fixed dose combination bilayer tablets for the treatment of tuberculosis. British Journal of Pharmaceutical Research 4 (14), 1781–1801. http://dx.doi.org/10.9734/BJPR/2014/11525.

Singh, S., Mariappan, T.T., Sharda, N., Kumar, S., Chakraborti, A.K., 2000. The reason for an increase in decomposition of rifampicin in the presence of isoniazid under acid conditions. Pharm. Pharmacol. Commun. 6 (9), 405–410. http://dx.doi.org/10.1211/146080800128736277.

Singh, Charan, Tara Datt Bhatt, Manjinder Singh Gill, and Sarasija Suresh. 2014. "Novel rifampicin-phospholipid complex for tubercular therapy: synthesis, physicochemical characterization and in-vivo evaluation." Int. J. Pharm. 460 (1–2). Elsevier B.V.: 220–227. http://dx.doi.org/10.1016/j.ijpharm.2013.10.043.

Son, Yoen Ju, and Jason T. McConville. 2011. "A New Respirable Form of Rifampicin." Eur. J. Pharm. Biopharm. 78 (3). Elsevier B.V.: 366–376. http://dx.doi.org/10.1016/j.ejpb.2011.02.004.

Telenti, A., Imboden, P., Marchesi, F., Lowrie, D., Cole, S., Colston, M.J., Matter, L., Schopfer, K., Bodmer, T., 1993. Detection of rifampicin-resistance mutations in mycobacterium tuberculosis. Lancet 341 (8846), 647–650. http://dx.doi.org/10.1016/0140-6736(93)90417-F.

The Japanese Pharmacopoeia, 1996. Tokyo: Society of Japanese Pharmacopoeia: Distributed by Yakuji Nippo.

U.S. Goverment Publishing Office, 2016. Electronix Code of Federal Regulations: Part 182—Substances Generally Recognized as Safe. http://www.ecfr.gov/cgi-bin/text-idx?c=ecfr&sid=3efaad1b0a259d4e48f1150a34d1aa77&rgn=div5&view=text&node=14:2.0.1.3.10&idno=14#14:2.0.1.3.10.3.7.6.

United States Pharmacopoeia, 2015. The National Formulary and Dispensing Information (USP 38-NF 33). USP, Rockville, MD.
Wang, Y., Liu, H., Liu, K., Sun, J., He, Z., 2013. Design and evaluation of enteric-coated tablets for rifampicin and isoniazid combinations. Pharm. Dev. Technol. 18 (2), 401–406. http://dx.doi.org/10.3109/10837450.2012.659254.
WHO, 2015. Tuberculosis|Fact Sheet N° 104. World Health Organization (doi:/entity/mediacentre/factsheets/fs104/es/index.html).
Yadav, V.B., Nigute, A.B., Yadav, A.V., Bhise, S.B., 2009. Enhancement of solubility and dissolution rate of rifampicin by melt granulation technique. J. Pharm. Res. 2 (2), 230–235.
Yan, Y.D., Sung, J.H., Kim, K.K., Kim, D.W., Kim, J.O., Lee, B.J., Yong, C.S., Choi, H.G., 2012. Novel valsartan-loaded solid dispersion with enhanced bioavailability and no crystalline changes. Int. J. Pharm. 422, 202–210.